

Implementation of a Misalignment-Tolerant MIMO Near Field Wireless Power Transfer System

Taroh Hijikata*, Allan Mesa Jr.[†], Charleston Dale Ambatali[‡]

Electrical and Electronics Engineering Institute

University of the Philippines Diliman

Quezon City, Philippines

*taroh.hijikata@eee.upd.edu.ph, [†]allan.jr.mesa@eee.upd.edu.ph, [‡]charleston.ambatali@eee.upd.edu.ph

Abstract—The efficiency of reactive near-field wireless power transfer (WPT) systems degrades rapidly with increasing separation distance and is highly sensitive to misalignment between transmitting and receiving coils. These limitations restrict the mobility of powered devices and confine many near-field WPT applications to static scenarios. To address these challenges, a multiple-input multiple-output (MIMO) WPT configuration is investigated due to its capability to shape the magnetic field distribution between the transmitter and receiver. Maximum power transfer efficiency can be achieved by appropriately setting the amplitude and phase of each transmitting coil; however, determining these optimal settings requires accurate knowledge of the system’s S-parameters. This paper presents the use of the Nelder-Mead iterative optimization algorithm to estimate the input amplitude and phase settings that maximize transfer efficiency in a near-field WPT system. The implementation comprises a four-element transmitter and a two-element receiver. Based on measured S-parameters, the proposed approach significantly improves WPT efficiency under both aligned and misaligned conditions.

Index Terms—wireless power transfer, near-field, misalignment tolerance.

I. INTRODUCTION

High-efficiency wireless power transfer (WPT) is achieved in the reactive or radiated near-field zones [14, 5]. Most commercial WPT products developed over the past decade use electromagnetic induction between two coils to transfer power over the air, typically to recharge smartphones that support wireless charging. However, for single-input single-output (SISO) inductive power transfer (IPT) systems, efficiency rapidly decreases as the distance between the transmitter and receiver increases [1].

In addition to distance-related issues, SISO IPT systems also suffer from misalignment sensitivity, causing rapid changes to the impedance seen by the power source and thereby reducing efficiency. This limits the operating conditions of the system, necessitating static relative positions between the source and receiver.

To address misalignment and distance issues, multiple coils can be used in different ways. One method is to use relay coils with mutual inductances tuned to accommodate a wide range of impedances [13]. Another is to use multiple coils as power sources [4], also called a multiple-input multiple-output (MIMO) IPT system. Techniques considered in long-range radiative WPT can be applied to MIMO-IPT. The

maximum theoretical efficiency can also be determined using the system’s S-parameters [15].

To determine the beam setting that achieves this (i.e., amplitude and phase setting of each coil), complete knowledge of the S-parameters is required for any given configuration. Due to the dynamic nature of contactless IPT, the computational complexity hinders the implementation of MIMO-IPT.

By treating the power transferred between coils as beams, dynamic beamforming solutions from radiative WPT can be implemented, known as dynamic beam focusing [6]. Previous work used a set of arbitrary focal points where the receiver was placed [5]. Others tracked receivers using directional radiation algorithms [7] or retrodirective antennas [3, 2, 9, 8].

In this paper, we present a particular MIMO-IPT implementation that utilizes the Nelder-Mead iterative optimization algorithm to determine the maximally efficient transmitter setting. The receiver coil reports its received power back to the transmitter coils, which then adjust amplitude and phase settings determined through the Nelder-Mead algorithm [12]. This process iterates until the received power converges. This removes dependency on estimating S-parameters, enabling practical use of MIMO-IPT. Furthermore, we show that MIMO-IPT is tolerant to misalignment, making it a promising candidate for contactless IPT.

II. MIMO-IPT IMPLEMENTATION

A. Coil Design and Board Fabrication

Assuming a constant Q-factor, transmission efficiency will reach 80% if the air gap is smaller than the coil radius [11]. Since the minimum operating distance of this work is set to 10 cm, the maximum diameter of the coil to be used is set to 20 cm. Fig.?? shows the geometric parameters of a square PSC. The parameters chosen for this implementation are number of turns $n = 2$, s and $w = 1$ cm, and $d_i = 14$ cm.

The fabricated PSC used FR4 as a substrate, with a board thickness of 1.6 mm, board dimensions of 24 cm x 24 cm, copper thickness t_c of 35 μm , and has 2 copper layers. An SMA port was used to serve as the input for the board, and test points were placed near the traces in order for an oscilloscope probe to capture the voltage of the input for the transmitter coils, and voltage at the load for the receiver coils. The capacitors used for the impedance matching networks

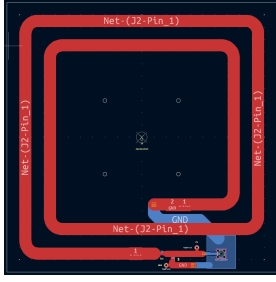


Fig. 1. The PSC in KiCAD 8.0

are surface mount device multilayer ceramic capacitors. The GERBER file of the PSC is shown in Fig.1.

B. Efficiency Prediction using S-parameters

Generally, given an M transmitter \times N receiver system, the relationship between the incident power wave and reflected power wave at all ports is given by an $(M + N) \times (M + N)$ S-parameter matrix. To calculate the maximum possible efficiency [15], the S-parameters of the system are used as expressed in equation (1).

$$\begin{bmatrix} \mathbf{B}_t \\ \mathbf{B}_r \end{bmatrix} = \begin{bmatrix} \mathbf{S}_{tt} & \mathbf{S}_{tr} \\ \mathbf{S}_{rt} & \mathbf{S}_{rr} \end{bmatrix} \begin{bmatrix} \mathbf{A}_t \\ \mathbf{A}_r \end{bmatrix} \quad (1)$$

In the above equation, $\mathbf{S}_{tt} \in \mathbb{C}^{M \times M}$ is the scattering matrix among the transmitters, $\mathbf{S}_{tr} \in \mathbb{C}^{M \times N}$ is the transfer matrix from receivers to transmitters, $\mathbf{S}_{rt} \in \mathbb{C}^{N \times M}$ is the transfer matrix from transmitters to receivers, and $\mathbf{S}_{rr} \in \mathbb{C}^{N \times N}$ is the scattering matrix among the receivers. $\mathbf{A}_t \in \mathbb{C}^{M \times 1}$ and $\mathbf{B}_t \in \mathbb{C}^{M \times 1}$ are the incident and reflected waves at the transmitters, respectively. $\mathbf{A}_r \in \mathbb{C}^{N \times 1}$ and $\mathbf{B}_r \in \mathbb{C}^{N \times 1}$ are the incident and reflected waves at the receivers, respectively. From equation (1), the maximum possible efficiency is determined using equation (2), where $()^T$ means matrix transpose, $()^*$ means complex conjugate, and $()^H$ means complex conjugate transpose, $\mathbf{A} = [\mathbf{A}_t \ \mathbf{A}_r]^T$ describes the incident waves on the coils, and \mathbf{E}_t and \mathbf{E}_r are the $M \times M$ and the $N \times N$ identity matrices, respectively.

$$\eta = -\frac{\mathbf{A}^H \mathbf{C} \mathbf{A}}{\mathbf{A}^H \mathbf{D} \mathbf{A}} \quad (2)$$

$$\mathbf{C} = \begin{bmatrix} \mathbf{S}_{tr}^* \mathbf{S}_{rt} & \mathbf{S}_{tr}^* \mathbf{S}_{rr} \\ \mathbf{S}_{rr}^* \mathbf{S}_{rt} & \mathbf{S}_{rr}^* \mathbf{S}_{rr} - \mathbf{E}_r \end{bmatrix}$$

$$\mathbf{D} = \begin{bmatrix} \mathbf{S}_{tt}^* \mathbf{S}_{tt} - \mathbf{S}_t & \mathbf{S}_{tt}^* \mathbf{S}_{tr} \\ \mathbf{S}_{rt}^* \mathbf{S}_{tt} & \mathbf{S}_{rt}^* \mathbf{S}_{tr} \end{bmatrix}$$

The expression for η above is the generalized Rayleigh quotient, with its maximum value derived from the generalized eigenvalue equation in(3), where γ are the $M + N$ eigenvalues and the columns of \mathbf{X} are the $M + N$ eigenvectors. The largest eigenvalue γ that is less than 1 is the maximum possible efficiency of the system. This serves as the baseline for evaluating the performance of the proposed iterative optimization setup.

$$\mathbf{C} \mathbf{X} = \gamma \mathbf{D} \mathbf{X} \quad (3)$$

C. Simulation and Implementation Setup

CST Studio Suite 2021 was used to simulate the S-parameters of the four-transmitter, two-receiver system. L-matching networks were employed to resonate all coils at 13.56 MHz. The goal of the impedance matching networks was to reduce self-reflection of all coils in the MIMO system at the operating frequency, thereby increasing overall efficiency.

The receivers were positioned 15 cm away and aligned with the transmitters. The values used for the L-matching networks are 120 pF series capacitors and 820 pF shunt capacitors. Fig.2a shows the single coil setup in CST while Fig.2b shows the MIMO setup.

The system's S-parameter matrix is exported to MATLAB for efficiency calculations. The maximum achievable efficiency was computed using equations (2) and (3). Simulations were carried out for different combinations of lateral misalignment and distance between transmitter and receiver coils. From the S-parameters, efficiency could be calculated for arbitrary settings.

The hardware implementation is shown in Fig.3 with block diagram in Fig.4. Signal generators and oscilloscopes were controlled via a computer through a USB interface using MATLAB. 50 Ω terminators served as the dummy load for the receivers.

Oscilloscopes captured waveforms, which were stored on the computer. FFT analysis was used to extract amplitude and phase information, forming complex numbers representing the total voltage of transmitters and receivers. The amplitude and phase set on the signal generators were used to construct the incident voltage of the transmitter. The incident voltage of the receiver was set to zero, so its total voltage equaled the reflected voltage. The reflected voltage of the transmitter was computed using $B_t = T_t - A_t$, where T_t is the total voltage of the transmitter.

D. Nelder-Mead Algorithm

Starting from an arbitrary initial setup denoted by \mathbf{A} , the Nelder-Mead algorithm [12] transforms the initial value of \mathbf{A} into a column vector that yields good efficiency whenever there is misalignment. Details of the algorithm is available in its original paper [12]. In summary, the algorithm begins with a

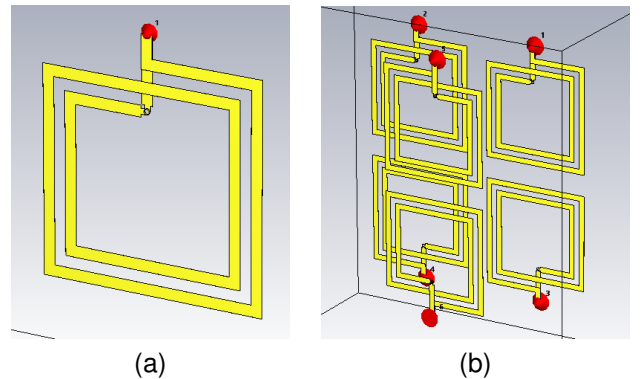


Fig. 2. (a) The 1 coil model and (b) the 4x2 coil model implemented in CST.

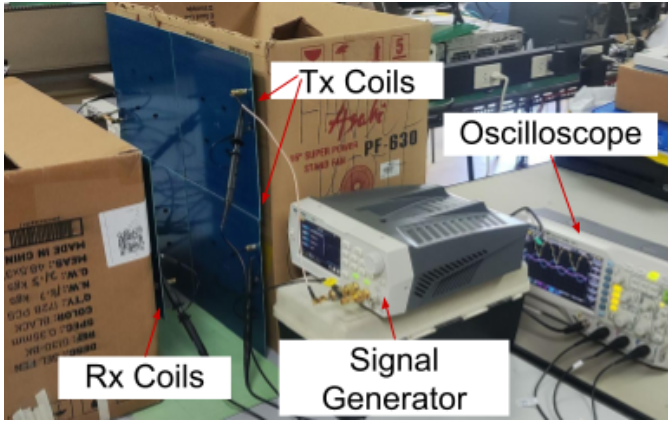


Fig. 3. Hardware measurement setup.

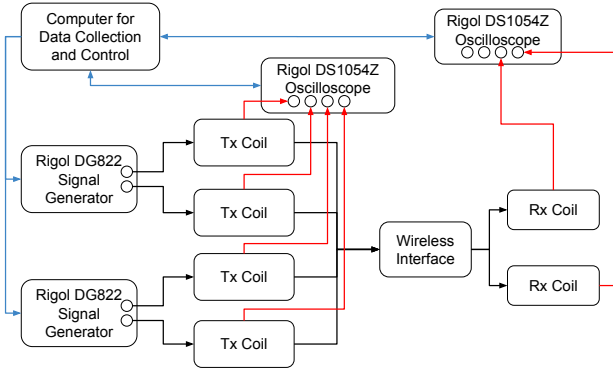


Fig. 4. Block diagram of the hardware

set of $n + 1$ vertices x_0, x_1, \dots, x_n , where n is the dimension, resulting in an initial working simplex S . Only the incident wave of the transmitter is optimized in A , resulting in $n = 8$.

The objective function $f(x)$ is evaluated at each vertex and arranged from lowest to highest. Since the goal is to maximize efficiency, the objective function used is the negative of equation (2). Centroid c is calculated using equation (4), assuming $f(0) \leq f(1) \leq \dots \leq f(n)$.

$$c = \frac{1}{n} \sum_{n=0}^{n-1} x_n \quad (4)$$

The worst-performing vertex is replaced depending on the location of c resulting in a new working simplex. The four transformations of the algorithm are reflection, expansion, contraction, and shrinking, relative to the best side. The reflection parameter α is set to 1, contraction parameter β is set to 0.5, expansion parameter γ is set to 2, and shrinking parameter δ is set to 0.5. If the smallest value of $f(x)$ converges, the iterations end. Else, the algorithm restarts again. This is summarized by the flowchart in Fig.5.

III. RESULTS AND DISCUSSIONS

For both the simulated and hardware systems, data were obtained at distances of 10 cm and 15 cm. The simulation

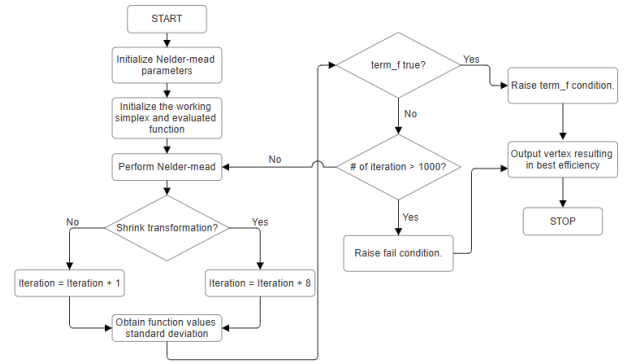


Fig. 5. Procedure for the algorithm

considered lateral misalignment in both the x-direction and y-direction, while the hardware setup considered misalignment only in the y-direction. In Fig.2b, the positive x-direction is to the right, and the positive y-direction is upward. Seven misalignment data points are considered from -30 cm to 30 cm. The input of all transmitters is set to an amplitude of 0.5 V and a phase of 0° for both the pre-Nelder-Mead setup and hardware. The Nelder-Mead algorithm is applied only to the simulated system and not in the hardware.

It must be noted that the power transfer efficiency being considered in this project is the beam efficiency, not the overall efficiency of the system.

Before applying Nelder-Mead, the simulated system at a distance of 10 cm achieved a maximum efficiency of 94.24%, at no misalignment. The lowest efficiency of the system in the y-direction is 76.61% and the lowest efficiency in the x-direction is 1.51%. After applying Nelder-Mead, the lowest efficiencies have improved from 76.61% to 93.92% and from 1.51% to 74.22%.

At a distance of 15 cm and before applying Nelder-Mead, the simulated system achieved a max efficiency of 91.92% at the case of no misalignment. The lowest efficiency in the y-direction is 78.37%, and 17.70% in the x-direction. After applying Nelder-Mead, efficiency of the system at all points has improved. Considering the worst points, 78.37% has improved to 91.45%, while 17.7% increased to 72.40%.

The simulated system was more tolerant to misalignment in the y-direction compared to the x-direction. Regardless of misalignment direction, efficiency was, on average, higher at a distance of 15 cm. This can be attributed to the impedance matching network being designed for a 15 cm distance with zero misalignment. The plots show that the Nelder-Mead algorithm greatly improves efficiency under large misalignment. Based on the project objectives, the simulated system is deemed misalignment-tolerant in the y-direction even without Nelder-Mead.

At a distance of 10 cm, the hardware system achieved a max efficiency of 92.51% at no misalignment and a minimum efficiency of 69.58% at -30 cm of misalignment. At a distance of 15 cm, the max efficiency is 90.63%, and the minimum efficiency is 64.52% at 30 cm of misalignment. The hardware

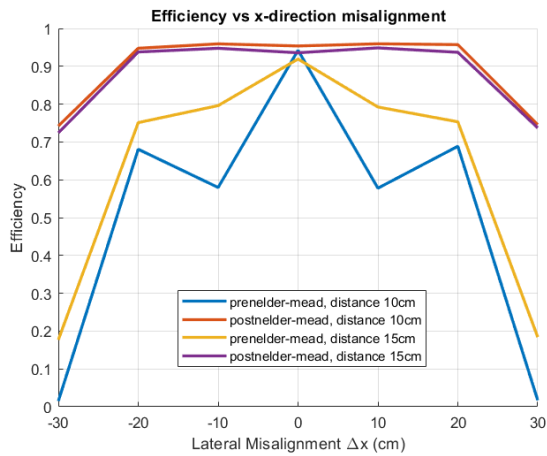


Fig. 6. Efficiency of the system vs x-direction misalignment

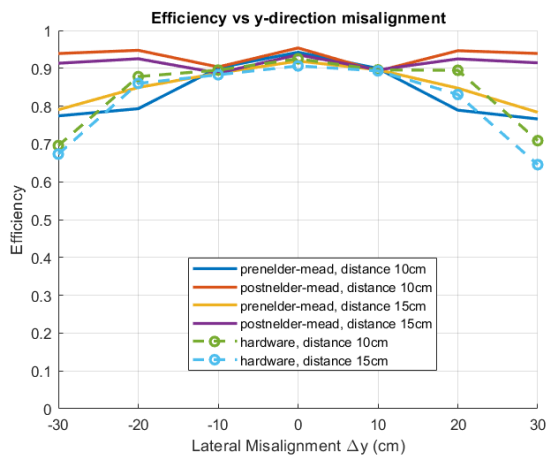


Fig. 7. Efficiency of the system vs y-direction misalignment

results also seem to be close to the simulation results, being slightly lower due to factors such as board losses, component losses, and instrument error. Although the input transmitter has the same amplitude and phases, from Fig.6, it can be seen that the efficiency of the hardware remained nearly flat from -20 cm to 20 cm before dipping at the maximum misalignment. Shown in Fig.6 is the plot of efficiency vs x-direction misalignment of the system while Fig.7 shows the plot of efficiency vs y-direction misalignment, including the measured results.

To analyze the S -parameter plots of the multiport network like a two-port network, the Frobenius norms of the submatrices in Eq. 1 are shown in Fig.8. The submatrices $S_{r,t}$ and $S_{t,r}$ describe the coupling between the transmitter array and the receiver array. This coupling is noticeable in the frequency range of 12.5 to 14.5 MHz.

The submatrices $S_{t,t}$ and $S_{r,r}$ represent the reflection losses and mutual coupling within the transmitter and receiver arrays, respectively. These submatrices do not have a frequency range where the Frobenius norm takes a very negative value; this "dip" is expected for a well-matched antenna array. These

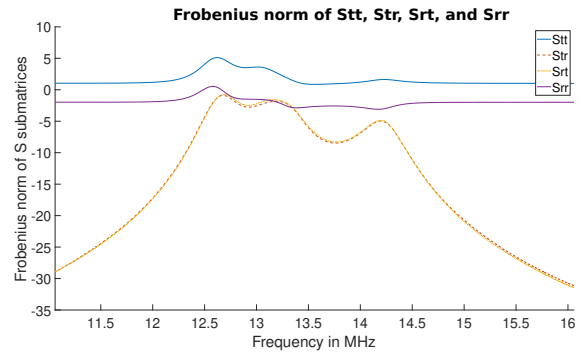


Fig. 8. Frobenius norm of S submatrices for system with separation of 15 cm, 0 misalignment

Frobenius norms suggest that some of the energy from transmitter element goes into other transmitter elements instead of a receiver element. Although beam efficiency could be improved by applying the Nelder-Mead algorithm, mutual coupling within both transmitter and receiver arrays is still observed.

IV. CONCLUSIONS AND RECOMMENDATIONS

From the results, both simulated and hardware systems are deemed misalignment-tolerant. The addition of the Nelder-Mead algorithm enhanced the simulated system's tolerance by improving efficiency under large misalignment. Even without the Nelder-Mead algorithm, both the simulated system and hardware remained misalignment-tolerant. This is attributed to the MIMO setup and the coils' ability to take advantage of resonance, maintaining efficient wireless power transfer.

For future work, it is highly recommended that decoupling networks [1, 10] be incorporated into the transmitters of this or any other MIMO setup. Decoupling networks can be implemented either by adding additional components or by introducing another layer of coils. To increase power output, the use of class E power amplifiers and rectifiers is also recommended.

ACKNOWLEDGMENT

We acknowledge the Office of the Chancellor of the University of the Philippines Diliman, through the Office of the Vice Chancellor for Research and Development, for funding support through the PhD Incentive Award Grant 252510 YEAR 1.

REFERENCES

- [1] Charleston Dale Ambatali and Shinichi Nakasuka. "Optimal Design of Decoupling Networks to Improve MIMO Microwave Wireless Power Transfer". In: *2024 IEEE Wireless Power Technology Conference and Expo (WPTCE)*. IEEE, 2024, pp. 261–265.
- [2] Charleston Dale Ambatali et al. "Experimental Validation of the Dynamics of the Both-Sides Retrodirective Antenna Array System". In: *2024 IEEE Wireless Power Technology Conference and Expo (WPTCE)*. 2024, pp. 132–136.
- [3] Charleston Dale M. Ambatali and Shinichi Nakasuka. "Characterizing the Dynamic Behavior of a Both-Sides Retrodirective System for the Control of Microwave Wireless Power Transfer". In: *2024 SICE International Symposium on Control Systems (SICE ISCS)*. 2024, pp. 99–106.

- [4] Quang-Thang Duong and Minoru Okada. "Maximum efficiency formulation for multiple-input multiple-output inductive power transfer systems". In: *IEEE transactions on microwave theory and techniques* 66.7 (2018), pp. 3463–3477.
- [5] Vinay R. Gowda et al. "Wireless Power Transfer in the Radiative Near Field". In: *IEEE Antennas and Wireless Propagation Letters* 15 (2016), pp. 1865–1868.
- [6] Ali Hajimiri et al. "Dynamic Focusing of Large Arrays for Wireless Power Transfer and Beyond". In: *IEEE Journal of Solid-State Circuits* 56.7 (2021), pp. 2077–2101.
- [7] Qi Hui, Ke Jin, and Xirui Zhu. "Directional Radiation Technique for Maximum Receiving Power in Microwave Power Transmission System". In: *IEEE Transactions on Industrial Electronics* 67.8 (2020), pp. 6376–6386.
- [8] Hinata Kato and Qiaowei Yuan. "Array Factor, Retrodirective, and E-MIMO Beamforming Technologies". In: *2023 IEEE International Symposium On Antennas And Propagation (ISAP)*. 2023, pp. 1–2.
- [9] Hyungmo Koo et al. "Retroreflective Transceiver Array Using a Novel Calibration Method Based on Optimum Phase Searching". In: *IEEE Transactions on Industrial Electronics* 68.3 (2021), pp. 2510–2520.
- [10] Allan Jose Mesa and Charleston Dale M Ambatali. "Multiport Pi-network Implementation of Decoupling Network for MIMO Wireless Power Transfer". In: *2025 IEEE Wireless Power Technology Conference and Expo (WPTCE)*. IEEE. 2025, pp. 1–4.
- [11] Xiaolin Mou et al. "Survey on magnetic resonant coupling wireless power transfer technology for electric vehicle charging". In: *IET Power Electronics* 12.12 (2019), pp. 3005–3020.
- [12] J. A. Nelder and R. Mead. "A Simplex Method for Function Minimization". In: *The Computer Journal* 7.4 (Jan. 1965), pp. 308–313. ISSN: 0010-4620. eprint: <https://academic.oup.com/comjnl/article-pdf/7/4/308/1013182/7-4-308.pdf>.
- [13] Cheng Peng et al. "Optimizing Wireless Power Transfer: Advanced Multi-Relay-Coil Design with Chebyshev Filter Theory". In: *2024 IEEE International Symposium on Antennas and Propagation and INC/USNC-URSI Radio Science Meeting (AP-S/INC-USNC-URSI)*. IEEE. 2024, pp. 1421–1422.
- [14] Naoki Shinohara. "Theory of WPT". In: *Wireless Power Transfer via Radiowaves*. John Wiley & Sons, 2014. Chap. 2, pp. 21–52.
- [15] Qiaowei Yuan. "S-Parameters for Calculating the Maximum Efficiency of a MIMO-WPT System: Applicable to Near/Far Field Coupling, Capacitive/Magnetic Coupling". In: *IEEE Microwave Magazine* 24.4 (2023), pp. 40–48.